



SRTTU

Journal of Computational and Applied Research
in Mechanical Engineering

jcarme.sru.ac.ir

JCARME

ISSN: 2228-7922

Research paper**Thermodynamic analysis of a hybrid absorption two-stage compression refrigeration system employing a flash tank with indirect subcooler****A. Emamifar****Mechanical Engineering Department, Ayatollah Boroujerdi University, P.O. Box: 69199-69411, Boroujerd, Iran***Article info:****Article history:**

Received: 12/11/2021

Accepted: 22/04/2022

Revised: 25/04/2022

Online: 27/04/2022

Keywords:

Cascade refrigeration

system,

Exergy,

Flash intercooler,

Subcooler.

***Corresponding author:**emamifar@abru.ac.ir**Abstract**

In this research, the thermodynamic analysis of a two-stage absorption compression refrigeration system employing a flash tank with indirect subcooler is presented. The absorption cycle uses LiBr-water solution as the working fluid and prepares the high temperature medium for the bottoming cycle, which is a two-stage compression refrigeration system with R744 refrigerant. The thermodynamic analysis indicates that the proposed system decreases the required electrical work and the total exergy destruction rate results in the improvement of the overall COP and total exergy efficiency. The results are compared with the same system without the subcooler and a simple cascade absorption compression refrigeration system. It was found that the overall COP and the total exergy efficiency of the proposed system are 7.86% and 11.21% higher than the system without the subcooler. These enhancements are 11.42% and 16.48% in comparison with the simple cascade absorption compression refrigeration system. Moreover, the effect of the generator temperature, condenser temperature, cascade condenser temperature, evaporator temperature, and the intermediate pressure of the compression section on the system electrical work, overall COP, total exergy destruction rate, and the total exergy efficiency of the proposed system are discussed.

1. Introduction

Reducing energy consumption has been a main problem in refrigeration systems. On the other hand, in recent years, increasing the demand for the energy resources, reduction the fossil fuels, and environmental concerns have been serious challenges in energy management systems [1-7]. Desirable refrigeration systems are those that consume low-grade energy and have optimized efficiency with less environmental impacts. To

reach these goals, integrating the refrigeration systems and cascade systems is considered as a promising solution to overcome the mentioned concerns [8-15]. Furthermore, in the applications with significant temperature differences, the cascade systems should be optimized, therefore, the multi-stage refrigeration systems and subcooling the refrigerants before throttling are developed [16-21]. In this way, many researchers have attempted to improve the performance of the cascade and hybrid

refrigeration cycles. Ratts and Brown [22] employed entropy analysis for a cascade cycle to determine the optimum intermediate temperature and pressure. They concluded that the cascade cycle losses reduced by 78% compared to the single cycle. Binging et al. [23] investigated the NH₃/CO₂ cascade refrigeration cycle and compared it with a two-stage and a single-stage NH₃ cycle. They concluded that the cascade system has the best COP for temperatures below -40°C. They also investigated the variations of different temperature parameters of the cycles on the performance of the system. Lee *et al.* [24] analyzed the first law and the second law equations for an NH₃/CO₂ cascade refrigeration system. They investigated the evaporator temperature, condenser temperature, and the DT cascade condenser on the performance of the cycle. Battacharyya and Sarkar [25] obtained optimum values for low, intermediate and, high temperatures for a two-stage CO₂/C₃H₈ cascade cycle. Getu and Bansal [26] carried out a thermodynamic analysis for an R744/R717 cascade refrigeration cycle and determined the optimum thermodynamic parameters for the system. Zubai *et al.* [27] analyzed a two-stage refrigeration cycle and concluded that the compressor efficiency causes the highest losses of the cycle. Ghorbani *et al.* [28] proposed a new integrated system of natural gas liquids, liquefied natural gas and, nitrogen remove unit and optimized it to reach the lower electrical power consumption. Mehrpooya *et al.* [29] introduced a novel system for large-scale NGL process using an absorption refrigeration system and reported a 31% and 30 % reduction in the heat transfer area and the power of the cycle, respectively. Torella *et al.* [30] presented a general method based on subcooling and desuperheating parameters related to seven two-stage refrigeration configurations and found the minimum COP for these systems. Rezayan and Behbahaninia [31] performed a thermodynamic optimization on a CO₂/NH₃ refrigeration cycle considering annual costs as the objective function. Aminyavari *et al.* [32] used a genetic algorithm for multi optimization of a CO₂/NH₃ cascade refrigeration cycle. The total cost and exergy efficiency were taken as the objective functions and, the optimum parameters were obtained. Eini *et al.* [33] presented a novel multi-objective optimization for a cascade

refrigeration cycle and introduced the optimum values based on the exergy, economic and inherent safety level of the system. Kilicarslan and Hosoz [34] analyzed the thermodynamic performance of a cascade refrigeration system and determined the couple refrigerants that have higher COP and lower irreversibility. Baakeem *et al.* [35] studied the performance of a multi-stage compression cycle for different refrigerants. They stated that R717 is an optimal refrigerant, while R407C is inadvisable as a refrigerant in the saturated system. Sun *et al.* [36] compared the thermodynamic performance of R23 and R41 in a cascade refrigeration system and concluded that using R41/RC404A in the system represents more desirable results in comparison with R23/R404A. Dopazo *et al.* [37] numerically and experimentally investigated a cascade refrigeration cycle employing CO₂ and NH₃ as the refrigerant. They obtained the optimum condenser temperature for CO₂ in the system. Ma *et al.* [38] used a falling film cascade heat exchanger in a refrigeration system. They stated that the smaller temperature difference of the proposed cascade heat exchanger improves the COP of the system. Sun *et al.* [39] investigated the best refrigerant couples for use in a cascade refrigeration cycle and recommended R170 and R41 for use in low-temperature cycles. They also introduced R161 for use in higher temperature cycles. Sarkar *et al.* [40] investigated proper natural refrigerant couples for a cascade refrigeration system based on normal boiling point and evaporator temperature. Manjili and Yavari [41] proposed a new CO₂ ejector refrigeration system using two intercoolers and concluded that multi-intercooling can improve COP in comparison with the conventional ejector refrigeration systems. Xing *et al.* [42] employed two ejectors in a two-stage CO₂ refrigeration cycle and demonstrated that compared with flash tanks, using double ejectors results in higher COP values. Mosaffa *et al.* [43] studied the parameters that enhance the performance and minimize the cost rates for two cascade refrigeration cycles with flash tank and investigated the effect of employing an indirect subcooler on system performance. Nemati *et al.* [44] compared the performance of using CO₂ and ethane in an ejector expansion refrigeration cycle in which the waste heat of the gas cooler was used in an ORC. Considering

thermodynamic parameters of the cycle, they concluded that ethane shows better performance as the refrigerant in their proposed cycle. Kumar Sing *et al.* [45] investigated a cascade refrigeration cycle that uses a flash tank in the high-temperature cycle and a flash tank with indirect subcooler in the low temperature cycle. They compared the results for different natural refrigerants. Ma *et al.* [46] investigated the effects of intercooling on heating performance for three different two-stage cycles and compared the heating performance for the sub-cycles of the presented systems. Mancuhan [47] investigated the use of flash intercooling in a refrigeration system for different refrigerants and proposed the optimum intermediate pressure for low and medium temperature applications.

Most of the studies on the cascade refrigeration systems employing a subcooler use different compression refrigeration cycles in upper and lower cycles. The focus of this paper is on employing an absorption system as a high temperature cycle in a hybrid cascade refrigeration system to save more electrical energy. The cold temperature cycle is a two-stage compression refrigeration system with a flash tank using an indirect subcooler. The system analysis is done using LiBr-water solution in the absorption section and a natural refrigerant R744 in the compression cycle. The analysis is performed based on the COP and exergy efficiency for different temperatures of evaporator, condenser, cascade condenser, generator, and different intermediate pressures of the compression section.

2. System description

Fig. 1 shows the schematics of a simple cascade absorption compression refrigeration system and a cascade absorption two-stage compression refrigeration system with a flash tank.

The schematic configuration of the proposed absorption two-stage compression cycle with a flash tank using the indirect subcooler is presented in Fig. 2.

The system consists of two refrigeration cycles. The low-temperature cycle (LTC) is a two-stage compression cycle employing a flash tank. The high-temperature cycle (HTC) is an absorption refrigeration cycle coupled with the LTC. The saturated liquid refrigerant entering the evaporator of the LTC absorbs heat from cold

space and evaporates. Compressor I superheats the refrigerant by increasing the pressure and temperature of the saturated refrigerant and discharges it into the flash tank, where there are some two-phase refrigerants. The superheat refrigerant cools down by rejecting heat to the saturated liquid refrigerant in the flash tank. Therefore, some of the liquid refrigerant in the flash tank vaporizes and mixes with the cooled superheat vapor so that the saturated vapor exits from the flash tank and flows through compressor II, where the second stage compressing occurs and the high pressure and temperature refrigerant discharges to the cascade condenser.

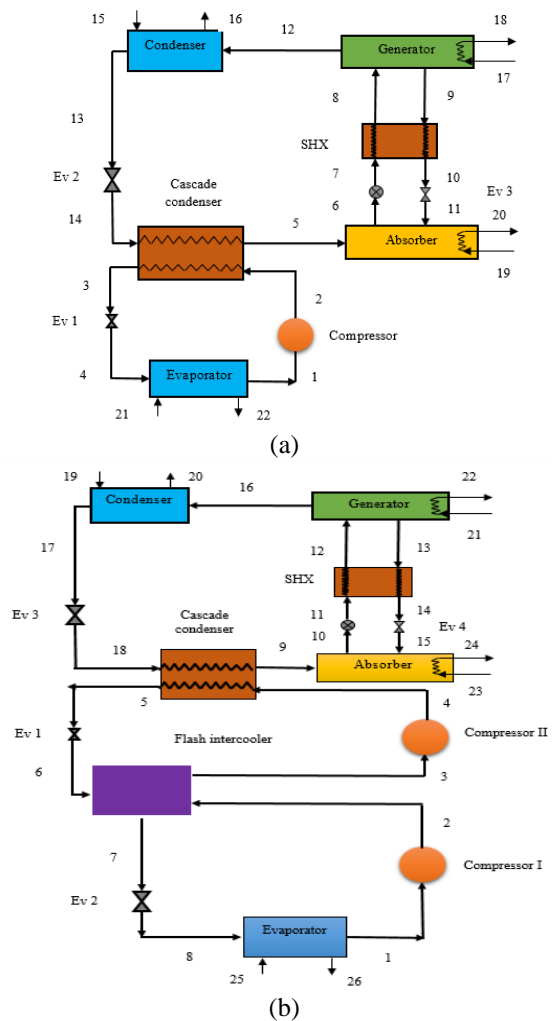


Fig. 1. (a) Simple cascade absorption compression cycle and (b) absorption two-stage compression cycle with a flash tank.

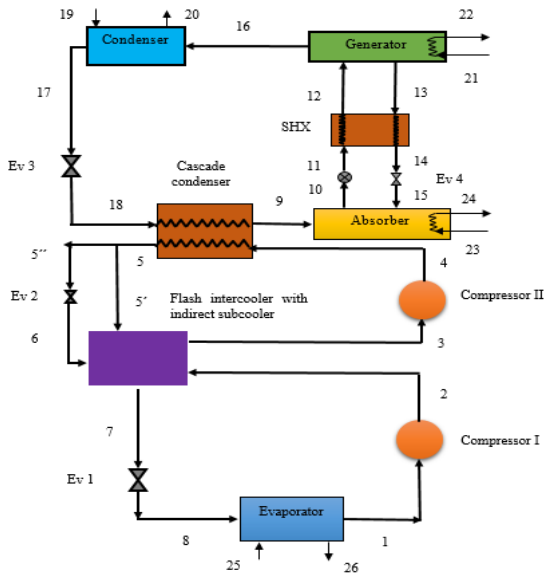


Fig. 2. Absorption two stage compression cycle with a flash tank using indirect subcooler.

In the cascade condenser, the superheat refrigerant rejects heat to the low-temperature water which comes from the absorption refrigeration system and condenses to the saturated liquid. The saturated liquid stream leaving the cascade condenser divides into two branches. One passes through the expansion valve 2 to reach the intermediate pressure and flows into the flash tank and, another stream gets subcooled passing through the flash tank. The cycle advances after passing the subcooled liquid refrigerant through the expansion valve 1 and entering the evaporator. The LiBr absorption refrigeration system in this study supplies the cooling fluid for the cascade condenser. The saturated water vapor leaving the cascade condenser enters the absorber, and mixes with the concentrated LiBr-H₂O solution (strong solution). So, a dilute LiBr-H₂O solution (weak solution) is obtained. The weak solution pumps to the generator passing through solution heat exchanger. The heat added to this weak solution in the generator separates the water vapor from the LiBr solution and makes the strong solution. This strong solution enters the absorber after passing through the solution heat exchanger and expansion valve. The pure water vapor leaving the generator enters the condenser, where it attains saturated liquid by rejecting heat to a low-temperature medium. The saturated liquid water then passes through the expansion valve and enters the evaporator.

3. Thermodynamic modeling

In order to investigate the thermodynamic performance of the system, the mass, energy, and exergy equations for the system should be analyzed. The EES software is employed in this study to perform all thermodynamic computations. The modeling of the proposed system is carried out based on the following assumptions:

- The steady-state operation is considered for the system;
- The temperature and the pressure losses through the pipes and equipment are neglected.
- The isenthalpic process occurs in all expansion valves;
- The states of the exit streams of the condensers, cascade condenser, and evaporator are saturated;
- The isentropic efficiency of the pump and compressors is constant.

The energy and exergy analysis of the system is performed applying the mass, the first law, and the second law of the thermodynamics on each component of the system. The mass equation for a steady-state system is given as:

$$\sum_k \dot{m}_{in} = \sum_k \dot{m}_{out} \quad (1)$$

Neglecting the kinetic and potential energies, the energy equation can be written as:

$$\dot{Q}_k + \sum_k (\dot{m}h)_{in} = \dot{W}_k + \sum_k (\dot{m}h)_{out} \quad (2)$$

In Eq. (2) \dot{W} , \dot{Q} , h_{in} , h_{out} and \dot{m} are the work rate, total heat transfer, mass flow rate, and inlet and outlet specific enthalpy for each system component. One of the serious challenges in refrigeration systems is the high rate of energy consumption. In the proposed system, the total necessary energy for the system can be obtained as:

$$\dot{W}_{tot} = \dot{W}_{compressorI} + \dot{W}_{compressorII} + \dot{W}_{pump} \quad (3)$$

The COP of the absorption system, compression system, and the total COP of the hybrid system can be defined as:

$$COP_{abs} = \frac{\dot{Q}_{cas}}{\dot{Q}_g + \dot{W}_p} \quad (4)$$

$$COP_{vc} = \frac{\dot{Q}_{evp}}{\dot{W}_{compressorI} + \dot{W}_{compressorII}} \quad (5)$$

$$COP_{total} = \frac{\dot{Q}_{evp}}{\dot{W}_{compressorI} + \dot{W}_{compressorII} + \dot{Q}_g + \dot{W}_p} \quad (6)$$

where, COP_{abs} , COP_{vc} , and COP_{total} are the coefficient of performance for the absorption system, compression system, and total system, respectively. Moreover, \dot{Q}_{cas} and \dot{Q}_g are the heat load of the cascade condenser and generator, respectively. Furthermore \dot{W}_p is the pump work. The intermediate pressure of the compression cycle is calculated as follows:

$$P_3 = \sqrt{P_1 P_4} \quad (7)$$

The degree of refrigerant subcooling in the compression cycle is derived as:

$$a = \frac{h_5 - h_8}{h_5 - h_6} \quad (8)$$

where h_6 is the enthalpy of the saturated liquid in the flash intercooler. $a=1$ reveals the maximum subcooling while $a=0$ denotes no subcooling.

Exergy analysis can eliminate some losses of the first law of thermodynamics. It can be useful to identify the cause of the system defects and improvement of the system's efficiency.

Neglecting the chemical exergy, the kinetic exergy and the potential exergy changes, the specific stream exergy is defined as:

$$\Psi = (h - h_0) - T_0 (s - s_0) \quad (9)$$

where h_0 and s_0 are the specific enthalpy and specific entropy of the fluid in the ambient temperature, respectively. T_0 is the surrounding temperature. The exergy destruction rates for various components of the system are presented in [Table 1](#). The net exergy destruction rate for the system can be calculated as:

$$\dot{I}_{dest} = \dot{E}x_{in} - \dot{E}x_{out} \quad (10)$$

The exergy efficiency of the system can be obtained as follows:

$$\eta_{II} = \frac{\dot{E}x_{out}}{\dot{E}x_{in}} = \frac{\dot{E}x_{in} - \dot{I}_{dest}}{\dot{E}x_{in}} = 1 - \frac{\dot{I}_{dest}}{\dot{E}x_{in}} \quad (11)$$

where, $\dot{E}x_{in}$ is the net electrical work inlet of the system plus the generator heat load; and $\dot{E}x_{out}$ is the exergy rate for cooling effect of the evaporator.

3. Model verification

In order to validate the absorption cycle modeling, the results of the absorption cycle have been compared with the numerical results reported by Florides et al. [17] with the following input parameters: $T_{gen} = 75^\circ\text{C}$, $T_{evp} = 6^\circ\text{C}$, $T_{cond} = 31.5^\circ\text{C}$, $T_{abs} = 34.9^\circ\text{C}$ and $Q_{evp} = 11$ kW. As can be seen in [Table 2](#), the maximum error in the numerical results is 1.61% for \dot{Q}_g .

The accuracy of the COP is about 1.35% which shows good agreement with the results of the Ref [17]. The bottoming cycle is validated with the theoretical results presented by Mancuhan [47] for a two stage flash intercooling refrigeration system, assuming the following input variables: $P_{int} = 593$ kPa, $T_{evp} = -20^\circ\text{C}$, $T_{cond} = 40^\circ\text{C}$, degree of subcooling=0 and degree of superheating=7°C. The comparison in single two stage flash intercooling CO₂ refrigeration system and the corresponding results of the Ref [47] are presented in [Table 3](#). As can be observed, there is small deviation between the results. The deviations are 7.11% for the COP and 3.91% for the exergy efficiency. Moreover, the comparison of the system COP variations versus condenser temperature with the Ref [47] is illustrated in [Fig. 3](#), which indicates good accuracy of the computations. The main input thermodynamic parameters of the system are presented in [Table 4](#).

Table 1. Energy and exergy equations for different components of the system.

Component	Energy equations	Exergy equations
Evaporator	$\dot{Q}_{evap} = \dot{m}_1(h_1 - h_8)$	$\dot{I}_{evap} = \dot{m}_8\psi_8 - \dot{m}_1\psi_1 + \dot{m}_{25}\psi_{25} - \dot{m}_{26}\psi_{26}$
Compressor I	$\dot{W}_{compressorI} = \dot{m}_1(h_2 - h_1)$	$\dot{I}_{comp} = \dot{m}_1\psi_1 - \dot{m}_2\psi_2 + \dot{W}_{compressorI}$
Compressor II	$\dot{W}_{compressorII} = \dot{m}_3(h_4 - h_3)$	$\dot{I}_{compA} = \dot{m}_3\psi_3 - \dot{m}_4\psi_4 + \dot{W}_{compressorII}$
	$\dot{m}_2 + \dot{m}_6 = \dot{m}_3$	
Flash intercooler	$\dot{m}_{5'} = \dot{m}_7$ $\dot{m}_5 h_{5'} + \dot{m}_6 h_6 + \dot{m}_2 h_2 = \dot{m}_7 h_7 + \dot{m}_3 h_3$	$I_{Flash} = \dot{m}_5\psi_{5'} + \dot{m}_6\psi_6 + \dot{m}_2\psi_2 - \dot{m}_7\psi_7 + \dot{m}_3\psi_3$
Expansion valve 1	$h_7 = h_8$ $\dot{m}_7 = \dot{m}_8$	$\dot{I}_{ev} = \dot{m}_7\psi_7 - \dot{m}_8\psi_8$
Expansion valve 2	$h_{5'} = h_6$ $\dot{m}_{5'} = \dot{m}_6$	$\dot{I}_{ev} = \dot{m}_5\psi_{5'} - \dot{m}_6\psi_6$
Cascade heat exchanger	$\dot{Q}_{cas} = \dot{m}_4(h_4 - h_5)$	$\dot{I}_{cas} = \dot{m}_4(\psi_4 - \psi_5) + \dot{m}_{18}(\psi_{18} - \psi_9)$
Expansion valve 3	$h_{17} = h_{18}$ $\dot{m}_{17} = \dot{m}_{18}$ $\dot{m}_9 + \dot{m}_{15} = \dot{m}_{10}$	$\dot{I}_{ev3} = \dot{m}_{17}\psi_{17} - \dot{m}_{18}\psi_{18}$
Absorber	$c_{15}\dot{m}_{15} = c_{10}\dot{m}_{10}$ $\dot{Q}_{abs} = \dot{m}_9 h_9 + \dot{m}_{15} h_{15} - \dot{m}_{10} h_{10}$ $\dot{W}_{pump} = \dot{m}_{10}(P_{16} - P_9) / \rho \eta_p$	$\dot{I}_{abs} = \dot{m}_9\psi_9 + \dot{m}_{15}\psi_{15} - \dot{m}_{10}\psi_{10} + \dot{m}_{23}\psi_{23} - \dot{m}_{24}\psi_{24}$
Pump	$\dot{W}_{pump} = \dot{m}_{11} h_{11} - \dot{m}_{10} h_{10}$ $\dot{m}_{11} = \dot{m}_{10}$ $\dot{m}_{11} h_{11} + \dot{m}_{13} h_{13} = \dot{m}_{12} h_{12} + \dot{m}_{14} h_{14}$	$\dot{I}_{pump} = \dot{m}_{10}\psi_{10} - \dot{m}_{11}\psi_{11} + \dot{W}_{pump}$
Solution heat exchanger	$\mathcal{E} = \frac{T_{13} - T_{14}}{T_{13} - T_{11}}$ $\dot{m}_{13} + \dot{m}_{16} = \dot{m}_{12}$	$\dot{I}_{She} = \dot{m}_{11}\psi_{11} + \dot{m}_{13}\psi_{13} - \dot{m}_{12}\psi_{12} - \dot{m}_{14}\psi_{14}$
Generator	$\dot{Q}_g = \dot{m}_{12} h_{12} - \dot{m}_{13} h_{13} - \dot{m}_{16} h_{16} = \dot{m}_{21} h_{21} - \dot{m}_{22} h_{22}$ $\dot{m}_{21} = \dot{m}_{22}$	$\dot{I}_{gen} = \dot{m}_{12}\psi_{12} - \dot{m}_{13}\psi_{13} - \dot{m}_{16}\psi_{16} + \dot{m}_{21}\psi_{21} - \dot{m}_{22}\psi_{22}$
Expansion valve 4	$h_{14} = h_{15}$ $\dot{m}_{14} = \dot{m}_{15}$	$\dot{I}_{ev4} = \dot{m}_{14}\psi_{14} - \dot{m}_{15}\psi_{15}$
Absorption Condenser	$\dot{Q}_{cond} = \dot{m}_{16} h_{16} - \dot{m}_{17} h_{17} = \dot{m}_{19} h_{19} - \dot{m}_{20} h_{20}$ $\dot{m}_{16} = \dot{m}_{17}, \dot{m}_{19} = \dot{m}_{20}$	$\dot{I}_{cond} = \dot{m}_{16}\psi_{16} - \dot{m}_{17}\psi_{17} + \dot{m}_{19}\psi_{19} - \dot{m}_{20}\psi_{20}$

Table 2. Comparison of the absorption cycle with Ref [17].

Parameter	Ref [17]	Present solution	Error (%)
\dot{Q}_a (kW)	14.1	13.95	1.06
\dot{Q}_{cond} (kW)	11.8	11.65	1.27
\dot{Q}_g (kW)	14.9	14.66	1.61
COP	0.74	0.75	1.35

Table 3. Comparison of the two stage compression cycle with Ref [47].

Parameter	Ref [47]	Present solution	Error (%)
\dot{W}_{total} kW)	2.36	2.2	6.7
η_{II} (%)	57.43	59.68	3.91
COP	2.53	2.71	7.11

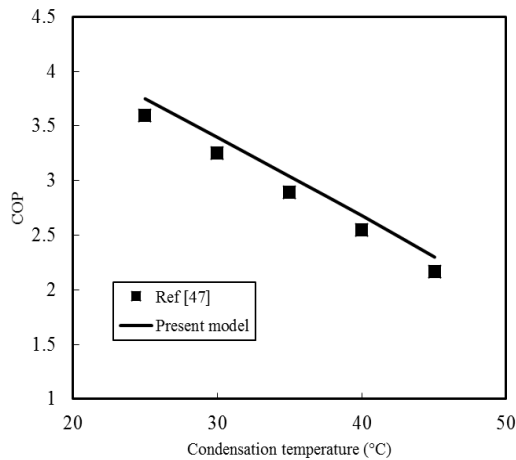


Fig. 3. Comparison of COP of the two-stage compression cycle versus condenser temperature with Ref [47].

3. Results and discussion

Tables 5 and 6 represent the energy and exergy related parameters of the proposed system (System 1), the system without a subcooler (System 2), and the simple cascade absorption compression refrigeration system (SCS). As can be observed, the total compressor work of the proposed system, the system without subcooler, and the SCS are 83.8 kW, 99.37 kW, and 106 kW, respectively; which demonstrate 15.66%, and 21% improvement for the proposed system compared to the system without subcooler and the SCS. The refrigerant quality after passing

through the expansion valve 1 reaches 0.1935 and 0.4208 for the proposed system and the system without subcooler, respectively. The quality of the refrigerant entering the evaporator for the SCS is 0.4229.

Table 4. The main input thermodynamic parameters of the system.

Parameter	Value
Absorber temperature (°C)	40
Absorber coolant inlet temperature (°C)	35
Absorber coolant outlet temperature (°C)	38
Condenser temperature (°C)	40
Condenser coolant inlet temperature (°C)	27
Condenser coolant outlet temperature (°C)	32
Generator temperature (°C)	90
Cascade condenser temperature difference (°C)	8
Intermediate pressure of the compression cycle (kPa)	2338
Subcooling parameter	0.9
Cooling capacity (kW)	200
Evaporator inlet air temperature (°C)	-20
Ambient temperature (°C)	25
Ambient Pressure (kPa)	101.325
Compressor isentropic efficiency	0.8
Solution heat exchanger efficiency	0.6

Table 5. Energy results of the system.

Parameter	System 1	System 2	SCS
\dot{Q}_{evap} (kW)	200	200	200
\dot{Q}_a (kW)	359.7	379.5	387.9
\dot{Q}_{cas} (kW)	283.8	299.4	306
\dot{Q}_{cond} (kW)	301.8	318.4	325.5
\dot{Q}_g (kW)	377.8	398.5	387.9
\dot{Q}_{shx} (kW)	51.4	54.22	55.42
COP_{total}	0.4333	0.4017	0.3896
$\dot{W}_{compressorI}$ (kW)	51.27	54.09	-
$\dot{W}_{compressorII}$ (kW)	32.52	45.29	-
$\dot{W}_{com(total)}$ (kW)	83.8	99.37	106

The lower quality of the refrigerant entering the evaporator increases the enthalpy difference through the evaporator. Considering the constant cooling capacity, the mass flow rate passing through the evaporator and consequently the required power of the compressor I decrease. Furthermore, the refrigerant enters compressor II and the SCS compressor at temperatures -14.1°C

and -40°C , respectively, which leads to lower compressor work in the proposed system compared to the SCS. Accordingly, using a flash intercooler with subcooler lowers the electrical work of the system, which leads to improving the total system COP by 7.86% and 11.21% in comparison with the flash intercooler system without a subcooler and the SCS, respectively. The exergy destruction values of System 1, System 2 and the SCS components are presented in Table 6.

As can be seen, the total exergy destruction of System 1 and System 2 is lower than the total exergy destruction of the SCS. The higher exergy destruction of the SCS is due to high values of exergy destructions in the evaporator, cascade condenser, compressor, and the expansion valve 2. In the SCS, the higher temperature difference through the expansion valve 2 and the cascade condenser, the higher enthalpy difference through the evaporator, the higher mass flow rate of the refrigerant, and the higher compressor work leads to an increase in the total exergy destruction in comparison with System 1 and System 2. The total exergy destructions for System 1, System 2 and the SCS are 97.21kW, 116.3kw, and 124.6kW, respectively. The lower exergy destruction in System 1 and System 2 results in 11.42% and 16.48% enhancement in the exergy efficiency for these systems compared to the flash intercooler system without subcooler and the SCS, respectively.

Fig. 4 shows the variations of the thermodynamic performance parameters of the system with intermediate pressure. As intermediate pressure increases, the COP of the system increases up to 2756 kPa and then declines for higher intermediate pressures. Increasing the intermediate pressure causes an increase in the pressure difference for compressor I and, on the contrary, decreases the pressure difference of compressor II. So there is an optimum value for the intermediate pressure, which minimizes the total electric work of the system. As it can be observed, increasing the intermediate pressure yields a similar trend for the exergy efficiency. In higher intermediate pressures, the decrement of exergy destruction of the compressor II, expansion valve 2 and, cascade condenser cannot compensate for the increment of the exergy destruction of the expansion valve 1, compressor I, and the flash tank.

Fig. 5 illustrates the variations of the energy and exergy parameters of the system for various amounts of temperature differences of the cascade condenser. By increasing the ΔT_{cas} , the exit temperature of compressor II increases, which results in increasing the corresponding saturation pressure, and consequently, the electric work done by compressor II increases. Moreover, in the higher ΔT_{cas} , the enthalpy difference of the compression side of the cycle increases, while the enthalpy difference of the absorption side, remains constant. Therefore, the mass flow rate of the absorption refrigerant increases, which causes an increase of more heat energy for the generator, and the system COP decreases. Furthermore, the exergy destruction of the cycle increases with increasing of the ΔT_{cas} . The main reason for this increment is the increase in the exergy destruction of the cascade condenser. By increasing the ΔT_{cas} from 8 to 18, \dot{Q}_g and $\dot{W}_{\text{compressorII}}$ increase about 17% and 58% which leads to 19.5% reduction of the system COP, respectively. Moreover, the exergy destruction rises about 54% by increasing the ΔT_{cas} from 8 to 18.

The effect of T_{evap} on thermodynamic performance of the system has been shown in Fig. 6. It is clear that with increasing the T_{evap} , the system COP and the exergy efficiency increase.

Table 6. Exergy results of the system.

Parameter	System 1	System 2	SCS
\dot{I}_a (kW)	21.92	23.12	23.63
\dot{I}_{evap} (kW)	5.112	5.115	5.208
\dot{I}_{cascade} (kW)	12.01	13.33	21.96
\dot{I}_{cond} (kW)	10.76	11.35	11.6
\dot{I}_g (kW)	12.96	13.67	13.98
\dot{I}_{SHX} (kW)	2.646	2.791	2.853
$\dot{I}_{\text{compressorI}}$ (kW)	7.111	7.501	-
$\dot{I}_{\text{compressorII}}$ (kW)	5.003	6.966	-
$\dot{I}_{\text{com(total)}}$ (kW)	12.114	14.467	17.51
\dot{I}_{Ev1} (kW)	7.569	26.74	26.97
\dot{I}_{Ev2} (kW)	4.53	2.307	-
\dot{I}_{Ev3} (kW)	0.79	0.8333	0.8515
\dot{I}_{FSH} (kW)	6.695	3.132	-
\dot{I}_{total} (kW)	97.21	116.3	124.6
η_{II} total	0.3844	0.345	0.33
\dot{E}_{in} (kW)	157.9	177.5	185.9

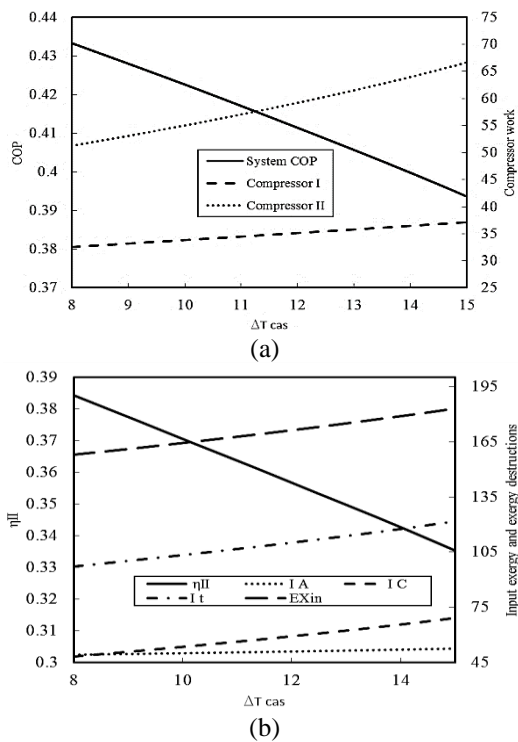


Fig. 5. Variations of the (a) COP and compressor works and (b) exergy efficiency, input exergy and exergy destructions with respect to ΔT_{cas} .

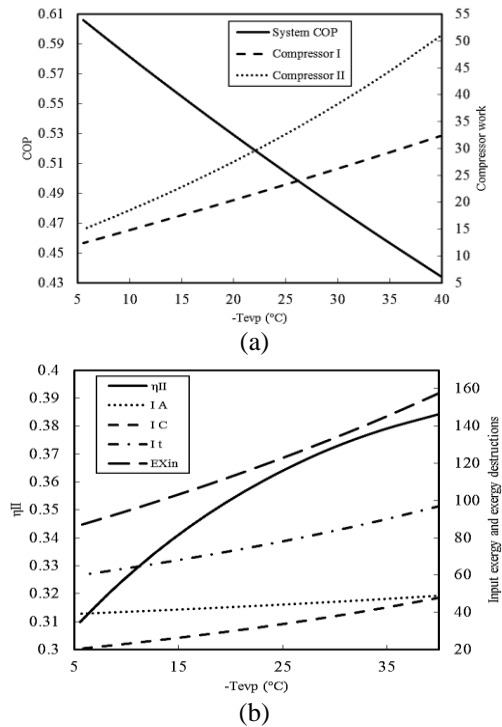


Fig. 6. Variations of the (a) COP and compressor works and (b) exergy efficiency, input exergy and exergy destructions with respect to evaporator temperature.

The reason is the decrease in total electrical work done by the compressors due to the reduction of the pressure difference of the cycle. Furthermore, by increasing the T_{evap} and subsequently decreasing the work demand for compressor I, the temperature at the exit of compressor I decreases, which leads to reducing the enthalpy difference for the compression section of the cascade condenser. As the temperature at the two sides of the absorption side of the cascade condenser is fixed, the mass flow rate of the absorption refrigerant decreases and reduces the generator heat input.

The reduction of the generator heat is another reason for reducing the COP of the system. By increasing the evaporator temperature, the exergy destruction of the absorption and the compression section of the cycle decreases. The most apparent reduction in exergy destruction occurs in the Ev1. In higher evaporator temperatures, the pressure loss through the Ev1 reduces, which causes a decrease in the exergy destruction. The reduction in the compressor works and mass flow rate of the absorption cycle refrigerant are the other considerable factors for reduction in the exergy destruction. However, the ratio of the exergy destruction to the inlet exergy is less for the lower evaporator temperatures so that the exergy efficiency increases.

The variations of the energy and exergy parameters of the system with cascade condenser temperature are depicted in Fig. 7. As it can be observed, increasing the cascade condenser temperature up to 6.67°C increases the total system COP and then declines. Referring to equation (6), the main parameters affecting the total system COP are \dot{Q}_g and \dot{W}_{tot} . Increasing the cascade condenser reduces the generator heat and increases the total electrical work for compressors. However, in temperatures higher than 6.67°C , the effect of compressor work increase is more preponderate than generator heat reduction, so the total system COP decreases. On the other hand, the COP of the compression section decreases due to the increase in the required electrical work. Since the reduction of the electrical work is superior to the reduction of the generator heat load, the lower cascade condenser temperatures are more desirable. By increasing the cascade condenser temperature, the exergy destruction of the

compression section increases while the exergy destruction of the absorption section almost remains constant. Hence the overall exergy destruction rate of the cycle increases, which lowers the exergy efficiency of the system. The effect of condenser temperature on thermodynamic performance of the system is shown in Fig. 8. By increasing the condenser temperature from 35°C to 40°C, the condenser pressure and consequently the generator pressure change from 5.627 kPa to 7.381 kPa. Whereas the temperature of the cascade condenser and the evaporator of the compression section are kept fixed, the variations of the condenser temperature do not affect the performance of the compression section. The solubility of water in LiBr solution increases with the increase of generator pressure, which leads to an increase in the circulation ratio, so the generator heat load increases by 2.86%. Hence, increasing the condenser temperature decreases the system COP.

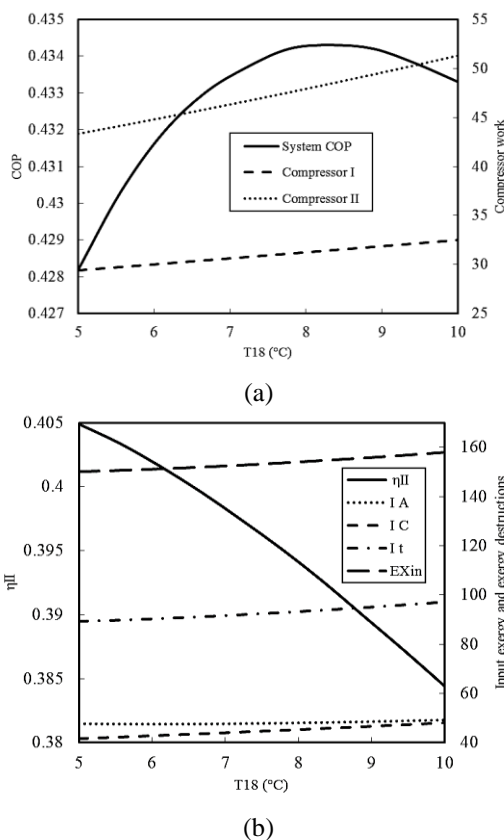


Fig. 7. Variations of the (a) COP and compressor works and (b) exergy efficiency, input exergy and exergy destructions with respect to cascade condenser temperature.

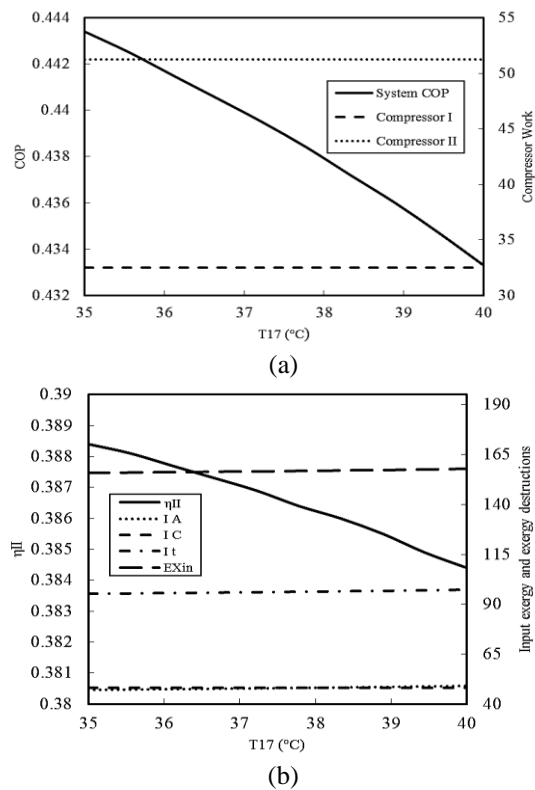


Fig. 8. Variations of the (a) COP and compressor works and (b) exergy efficiency, input exergy and exergy destructions with respect to condenser temperature.

Moreover, increasing the condenser temperature leads to increasing the temperature difference for the condenser and external cooling fluid, which increases the irreversibility of the condenser. Hence, the exergy efficiency of the cycle decreases by 0.94% with this temperature rise. Fig. 9 plots the variations of the energy and exergy parameters of the system with generator temperature. It can be found from this figure that increasing T_g firstly rises the system COP, and then it remains constant. By increasing the generator temperature, the solubility of water in LiBr solution decreases, which results in a decrease in the circulation ratio and consequently the heat load of the generator. So the absorption section COP increases. However, with more increment in the generator temperature, the rate of solubility of the refrigerant in LiBr solution becomes continuously smaller, which leads to diminishing the decrease rate of the circulation ratio and generator heat load. So the system COP approaches a constant value.

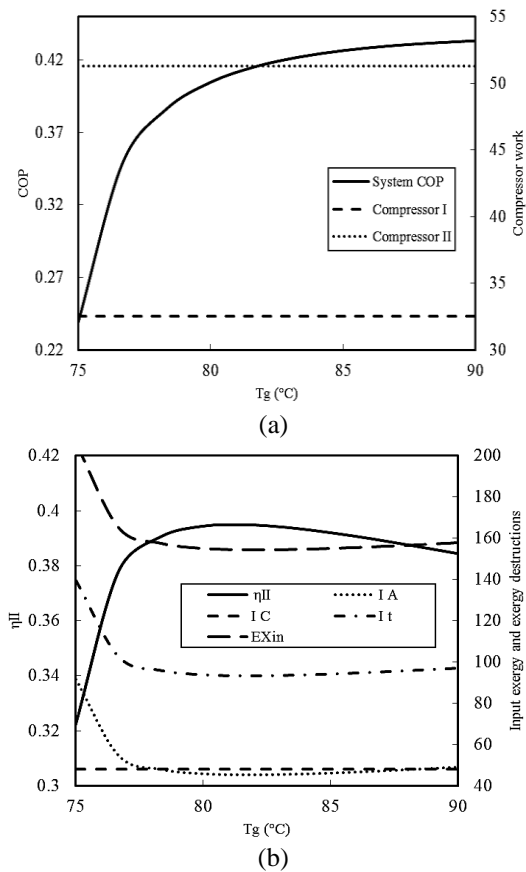


Fig. 9. Variations of the (a) COP and compressor works and (b) exergy efficiency, input exergy and exergy destructions with respect to generator temperature.

The exergy efficiency shows the same behavior as the system COP with increasing the generator temperature. In lower generator temperatures, the exergy entering the system is high to supply sufficient energy for evaporating the refrigerant in the generator. When T_g continues to rise, the temperature of the heat source increases, and the exergy difference between inlet and outlet temperatures of the external liquid increases, which leads to an increase in the inlet exergy of the system. Moreover, the irreversibility of the generator increases with more increasing of the heat source temperature.

3. Conclusions

In this work, the thermodynamic analysis is carried out for an absorption two-stage compression cycle equipped with a flash tank. The effect of subcooling the refrigerant in the flash tank is investigated and the results are

compared with a simple cascade absorption compression cycle. The proposed cycle enhances the COP and the exergy efficiency of the system by 7.86% and 11.21 % in comparison with the system without a subcooler. The enhancement for the COP and the exergy efficiency are 11.42% and 16.48% compared to a simple cascade absorption compression refrigeration system. The most important contributions of the parametric study investigation are as follows:

- There is an optimum value for the intermediate pressure of the compression cycle, which maximizes the COP and the exergy efficiency.
- Increasing the ΔT_{cas} increases the compressor works of the compression cycle and the exergy destruction of the cascade condenser, so the COP and the exergy efficiency decrease with increasing the ΔT_{cas} .
- In higher evaporator temperatures, the electrical work done by the compressors decreases which causes an increase in the COP of the system. Moreover, decreasing the exergy destruction of the Ev2 and the mass flow rate of the absorption cycle can be observed in the higher evaporator temperatures. However the higher ratio of the exergy destruction to the inlet exergy at lower evaporator temperatures increases the exergy efficiency of the cycle.
- Increasing the cascade condenser temperature reduces the generator heat and increases the total electrical work of the compressors. However, in temperatures higher than 6.67°C the effect of compressor work increase is more considerable which reduces the COP of the system. In higher cascade condenser temperatures, the exergy destruction of the compression section increases, while the exergy destruction of the absorption section almost remains constant. Hence the total exergy destruction of the cycle increases.
- By increasing the condenser temperature from 35°C to 40°C, the generator heat load increases by 2.86%. Hence, increasing the condenser temperature decreases the system COP. This temperature rise decreases the exergy efficiency of the system by 0.98%.
- By increasing the generator temperature, the circulation ratio, and consequently the heat load of the generator decreases, the COP of the system increases. The exergy efficiency shows the same behavior like the system COP with increasing the generator temperature.

References

- [1] Y. T. Ge, S. A. Tassou, I. Chaer and N. Suguartha, "Performance evaluation of a tri-generation system with simulation and experiment," *Appl. Energy.*, Vol. 86, No. 11, pp. 2317-2326, (2009).
- [2] P. Jakończuk, K. Śmierciew, H. Zou, D. Butrymowicz and A. Dudar, "Temperature drop of heating fluid as a primary condition for effective utilization of low-grade heat using flash cycles and zeotropic mixtures in refrigeration ejector systems," *Energy Sources Part A.*, pp. 1-19, (2021).
- [3] S. M. H. Mohammadi and M. Ameri, "Energy and exergy analysis of absorption-compression hybrid air-conditioning system," *HVAC&R Research*, Vol. 19, No. 6, pp. 744-753, (2013).
- [4] M. Mohanraj, S. Jayaraj and C. Muraleedharan, "Environment friendly alternatives to halogenated refrigerants—A review," *Int. J. Greenhouse Gas Control.*, Vol. 3, No. 1, pp. 108-119, (2009).
- [5] P. Soni, A. Sur, V. K. Gaba and R. P. Sah, "Review on improvement of adsorption refrigeration systems performance using composite adsorbent: current state of art," *Energy Sources Part A.*, pp. 1-25, (2021).
- [6] J. Alinejad, "Lattice Boltzmann simulation of a fluid flow around a triangular unit of three isothermal cylinders," *J. Appl. Mech. Tech. Phys.*, Vol. 57, No. 1, pp. 117-126, (2016).
- [7] J. Alinejad and J. A. Esfahani, "Lattice Boltzmann simulation of 3-dimensional natural convection heat transfer of CuO/water nanofluids," *Thermophys. Aeromech.*, Vol. 24, No. 1, pp. 95-108, (2017).
- [8] Ashwni, A. F. Sherwani, D. Tiwari and A. Kumar, "Sensitivity analysis and multi-objective optimization of organic Rankine cycle integrated with vapor compression refrigeration system," *Energy Sources Part A.*, pp. 1-13, (2021).
- [9] C. Cimsit and I. T. Ozturk, "Analysis of compression-absorption cascade refrigeration cycles," *Appl. Therm. Eng.*, Vol. 40, pp. 311-317, (2012).
- [10] Y. Fan, L. Luo and B. Souyri, "Review of solar sorption refrigeration technologies: Development and applications," *Renewable Sustainable Energy Rev.*, Vol. 11, No. 8, pp. 1758-1775, (2007).
- [11] J. Fernández-Seara, J. Sieres and M. Vázquez, "Compression-absorption cascade refrigeration system," *Appl. Therm. Eng.*, Vol. 26, No. 5, pp. 502-512, (2006).
- [12] W. Han, L. Sun, D. Zheng, H. Jin, S. Ma and X. Jing, "New hybrid absorption-compression refrigeration system based on cascade use of mid-temperature waste heat," *Appl. Energy.*, Vol. 106, pp. 383-390, (2013).
- [13] M. Wang, T. M. Becker, B. A. Schouten, T. J. H. Vlught and C. A. Infante Ferreira, "Ammonia/ionic liquid based double-effect vapor absorption refrigeration cycles driven by waste heat for cooling in fishing vessels," *Energy Convers. Manage.*, Vol. 174, pp. 824-843, (2018).
- [14] J. Alishah, S. Maddah, J. Alinejad and Y. Rostamiyan, "3D numerical simulation of flap geometry optimization around the cylinder to collection of split up droplet," *Fluid Dyn. Res.*, Vol. 53, No. 4, p. 045504, (2021).
- [15] M. M. Peiravi and J. Alinejad, "Nano particles distribution characteristics in multi-phase heat transfer between 3D cubical enclosures mounted obstacles," *Alexandria Eng. J.*, Vol. 60, No. 6, pp. 5025-5038, (2021).
- [16] G. Cacciola, G. Restuccia and G. Rizzo, "Theoretical performance of an absorption heat pump using ammonia-water-potassium hydroxide solution," *Heat Recovery Syst. CHP.*, Vol. 10, No. 3, pp. 177-185, (1990).

- [17] G. A. Florides, S. A. Kalogirou, S. A. Tassou and L. C. Wrobel, "Modelling, simulation and warming impact assessment of a domestic-size absorption solar cooling system," *Applied Thermal Engineering*, Vol. 22, No. 12, pp. 1313-1325, (2002).
- [18] P. Srihirin, S. Aphornratana and S. Chungpaibulpatana, "A review of absorption refrigeration technologies," *Renewable Sustainable Energy Rev.*, Vol. 5, No. 4, pp. 343-372, (2001).
- [19] I. Dincer and M. Kanoglu, "Refrigeration System Components," in *Refrigeration Systems and Applications*, pp. 105-153, (2010).
- [20] M. M. Peiravi, J. Alinejad, d. ganji and s. maddah, "Numerical study of fins arrangement and nanofluids effects on three-dimensional natural convection in the cubical enclosure," (in en), *Chall. Nano Micro Scale Sci. Tech.*, Vol. 7, No. 2, pp. 97-112, (2019).
- [21] M. M. Peiravi, J. Alinejad, D. D. Ganji and S. Maddah, "3D optimization of baffle arrangement in a multi-phase nanofluid natural convection based on numerical simulation," *Int. J. Numer. Methods Heat Fluid Flow.*, Vol. 30, No. 5, pp. 2583-2605, (2020).
- [22] E. B. Ratts and J. S. Brown, "A generalized analysis for cascading single fluid vapor compression refrigeration cycles using an entropy generation minimization method," *Int. J. Refrig.*, Vol. 23, No. 5, pp. 353-365, (2000).
- [23] W. Bingming, W. Huagen, L. Jianfeng and X. Ziwen, "Experimental investigation on the performance of NH₃/CO₂ cascade refrigeration system with twin-screw compressor," *Int. J. Refrig.*, Vol. 32, No. 6, pp. 1358-1365, (2009).
- [24] T.-S. Lee, C.-H. Liu and T.-W. Chen, "Thermodynamic analysis of optimal condensing temperature of cascade-condenser in CO₂/NH₃ cascade refrigeration systems," *Int. J. Refrig.*, Vol. 29, No. 7, pp. 1100-1108, (2006).
- [25] S. Bhattacharyya, S. Bose and J. Sarkar, "Exergy maximization of cascade refrigeration cycles and its numerical verification for a transcritical CO₂-C₃H₈ system," *Int. J. Refrig.*, Vol. 30, No. 4, pp. 624-632, (2007).
- [26] H. M. Getu and P. K. Bansal, "Thermodynamic analysis of an R744-R717 cascade refrigeration system," *Int. J. Refrig.*, Vol. 31, No. 1, pp. 45-54, (2008).
- [27] S. M. Zubair, M. Yaqub and S. H. Khan, "Second-law-based thermodynamic analysis of two-stage and mechanical-subcooling refrigeration cycles," *Int. J. Refrig.*, Vol. 19, No. 8, pp. 506-516, (1996).
- [28] B. Ghorbani, M.-H. Hamed, M. Amidpour and M. Mehrpooya, "Cascade refrigeration systems in integrated cryogenic natural gas process (natural gas liquids (NGL), liquefied natural gas (LNG) and nitrogen rejection unit (NRU))," *Energy*, Vol. 115, pp. 88-106, (2016).
- [29] M. Mehrpooya, M. Omid and A. Vatani, "Novel mixed fluid cascade natural gas liquefaction process configuration using absorption refrigeration system," *Appl. Therm. Eng.*, Vol. 98, pp. 591-604, (2016).
- [30] E. Torrella, J. A. Larumbe, R. Cabello, R. Llopis and D. Sanchez, "A general methodology for energy comparison of intermediate configurations in two-stage vapour compression refrigeration systems," *Energy*, Vol. 36, No. 7, pp. 4119-4124, (2011).
- [31] O. Rezayan and A. Behbahaninia, "Thermoeconomic optimization and exergy analysis of CO₂/NH₃ cascade refrigeration systems," *Energy*, Vol. 36, No. 2, pp. 888-895, (2011).
- [32] M. Aminyavari, B. Najafi, A. Shirazi and F. Rinaldi, "Exergetic, economic and environmental (3E) analyses, and multi-objective optimization of a CO₂/NH₃ cascade refrigeration system," *Appl. Therm. Eng.*, Vol. 65, No. 1, pp. 42-50, (2014).

- [33] S. Eini, H. Shahhosseini, N. Delgarm, M. Lee and A. Bahadori, "Multi-objective optimization of a cascade refrigeration system: Exergetic, economic, environmental, and inherent safety analysis," *Appl. Therm. Eng.*, Vol. 107, pp. 804-817, (2016).
- [34] A. Kilicarslan and M. Hosoz, "Energy and irreversibility analysis of a cascade refrigeration system for various refrigerant couples," *Energy Convers. Manage.*, Vol. 51, No. 12, pp. 2947-2954, (2010).
- [35] S. S. Baakeem, J. Orfi and A. Alabdulkarem, "Optimization of a multistage vapor-compression refrigeration system for various refrigerants," *Appl. Therm. Eng.*, Vol. 136, pp. 84-96, (2018).
- [36] Z. Sun *et al.*, "Comparative analysis of thermodynamic performance of a cascade refrigeration system for refrigerant couples R41/R404A and R23/R404A," *Appl. Energy*, Vol. 184, pp. 19-25, (2016).
- [37] J. Alberto Dopazo, J. Fernández-Seara, J. Sieres and F. J. Uhía, "Theoretical analysis of a CO₂-NH₃ cascade refrigeration system for cooling applications at low temperatures," *Appl. Therm. Eng.*, Vol. 29, No. 8, pp. 1577-1583, (2009).
- [38] M. Ma, J. Yu and X. Wang, "Performance evaluation and optimal configuration analysis of a CO₂/NH₃ cascade refrigeration system with falling film evaporator-condenser," *Energy Convers. Manage.*, Vol. 79, pp. 224-231, (2014).
- [39] Z. Sun, Q. Wang, Z. Xie, S. Liu, D. Su and Q. Cui, "Energy and exergy analysis of low GWP refrigerants in cascade refrigeration system," *Energy*, Vol. 170, pp. 1170-1180, (2019).
- [40] J. Sarkar, S. Bhattacharyya and A. Lal, "Selection of suitable natural refrigerants pairs for cascade refrigeration system," *Proc. Inst. Mech. Eng., Part A: J. Power Energy*, Vol. 227, No. 5, pp. 612-622, (2013).
- [41] F. E. Manjili and M. A. Yavari, "Performance of a new two-stage multi-intercooling transcritical CO₂ ejector refrigeration cycle," *Appl. Therm. Eng.*, Vol. 40, pp. 202-209, (2012).
- [42] M. Xing, J. Yu and X. Liu, "Thermodynamic analysis on a two-stage transcritical CO₂ heat pump cycle with double ejectors," *Energy Convers. Manage.*, Vol. 88, pp. 677-683, (2014).
- [43] A. H. Mosaffa, L. G. Farshi, C. A. Infante Ferreira and M. A. Rosen, "Exergoeconomic and environmental analyses of CO₂/NH₃ cascade refrigeration systems equipped with different types of flash tank intercoolers," *Energy Convers. Manage.*, Vol. 117, pp. 442-453, (2016).
- [44] A. Nemat, R. Mohseni and M. Yari, "A comprehensive comparison between CO₂ and Ethane as a refrigerant in a two-stage ejector-expansion transcritical refrigeration cycle integrated with an organic Rankine cycle (ORC)," *J. Supercrit. Fluids*, Vol. 133, part 1, pp. 494-502, (2018).
- [45] K. Kumar Singh, R. Kumar and A. Gupta, "Comparative energy, exergy and economic analysis of a cascade refrigeration system incorporated with flash tank (HTC) and a flash intercooler with indirect subcooler (LTC) using natural refrigerant couples," *Sustainable Energy Technol. Assess.*, Vol. 39, p. 100716, (2020).
- [46] J. Ma, A. Mhanna, N. Juan, M. Brands and A. S. Fung, "Effects of Intercooling and Inter-Stage Heat Recovery on the Performance of Two-Stage Transcritical

- CO₂ Cycles for Residential Heating Applications," *Energies*, Vol. 12, No. 24, p. 4763, (2019).
- [47] E. Mancuhan, "A comprehensive comparison between low and medium temperature application refrigerants at a two-stage refrigeration system with flash intercooling," *Therm. Sci. Eng. Prog.*, Vol. 13, p. 100357, (2019).

Copyrights ©2021 The author(s). This is an open access article distributed under the terms of the Creative Commons Attribution (CC BY 4.0), which permits unrestricted use, distribution, and reproduction in any medium, as long as the original authors and source are cited. No permission is required from the authors or the publishers.



How to cite this paper:

A. Emamifar, "Thermodynamic analysis of a hybrid absorption two-stage compression refrigeration system employing a flash tank with indirect subcooler", *J. Comput. Appl. Res. Mech. Eng.*, Vol. 12, No. 2, pp. 145-159, (2023).

DOI: 10.22061/JCARME.2022.8591.2154

URL: https://jcarme.sru.ac.ir/?_action=showPDF&article=1700

